TIME-DEPENDENT SEISMIC HAZARD IN THE SAN FRANCISCO BAY REGION, CALIFORNIA

Ivan Wong[1], Patricia Thomas[2], and Robert Youngs[3]

[1] *Principal Seismologist/Vice President, Seismic Hazards Group, URS Corporation, Oakland, California, USA*
[2] *Project Earthquake Engineer, Seismic Hazards Group, URS Corporation, Oakland, California, USA*
[3] *Principal Engineer, Geomatrix Consultants, Inc., Oakland, California, USA*
Email: ivan_wong@urscorp.com

ABSTRACT:

A key assumption in standard probabilistic seismic hazard analysis (PSHA) is that earthquake occurrence can be modeled as a Poisson process (time-independent). For but a few regions in the world, however, the timing information on past earthquakes are not sufficient to calculate time-dependent hazard. We have calculated time-dependent probabilistic hazard for the San Francisco Bay region (SFBR) resulting from the region's seven major faults (e.g., San Andreas, Hayward-Rodgers Creek) using the range of models that were considered by the Working Group on California Earthquake Probabilities (WGCEP, 2003). Based on their results, there is an increasing probability of a large (moment magnitude [**M**] > 6.7) earthquake occurring in the SFBR in the period 2002 to 2031. The estimated probability in 2002 was 62%. WGCEP (2003) considered five probability models that take into account various degrees of physics, date of last rupture, recent seismicity rates, and slip in the 1906 **M** 7.9 San Francisco earthquake. The probability models, which are not all time-dependent, and their weights were used to compute the rates of characteristic events for each rupture source in the WGCEP (2003) model. These rates were then input into the PSHA code, along with the source geometries, characteristic magnitudes, and shape of the magnitude distributions. All other faults in the seismic source model are treated in a time-independent manner. The probabilistic hazard was calculated for the cities of San Francisco, Oakland, and San Jose to evaluate the sensitivities of the hazard in the SFBR to parameters of the WGCEP (2003) model. The difference between the time-dependent and time-independent hazard depends on the proximity to the major faults. For example, a site in San Francisco along the San Andreas fault shows little difference in the two types of hazard because of the recent occurrence of the 1906 earthquake. In contrast, a site in Oakland located adjacent to the Hayward fault shows a 5 to 10% higher time-dependent hazard because the average recurrence interval has nearly elapsed.

KEY WORDS: Time-dependent probabilistic hazard, San Francisco Bay region, San Andreas fault system

1. INTRODUCTION

The probabilistic seismic hazard analysis (PSHA) approach is a standard practice in the engineering seismology/earthquake engineering community. The PSHA methodology allows for the explicit consideration of epistemic uncertainties and inclusion of the range of possible interpretations of components in the seismic hazard model, including seismic source characterization and ground motion estimation. Uncertainties in models and parameters can be incorporated into PSHA through the use, for example, of logic trees.

A key assumption of the standard PSHA model is that earthquake occurrences can be modeled as a Poisson time-independent process. The occurrence of ground motions at a site in excess of a specified level is also a Poisson process, if (1) the occurrence of earthquakes is a Poisson process, and (2) the probability that any one event will result in ground motions at the site in excess of a specified level is independent of the occurrence of other events. In a departure from standard PSHA, we have calculated time-dependent hazard in the San Francisco Bay region (SFBR) using the range of models for the major Bay Area faults that were considered by the U.S. Geological Survey's (USGS) Working Group on California Earthquake Probabilities study entitled "Earthquake Probabilities in the San Francisco Bay Region: 2002-2031" (WGCEP, 2003). Based on those results, there is an increasing probability of a large (moment magnitude [**M**] ≥ 6.7) earthquake occurring in the SFBR in the period 2002 to 2031. The estimated probability in 2002 was 62%. The highest probability of any individual fault was 27% for the Hayward-Rodgers Creek fault (WGCEP, 2003).

The following describes our estimates of time-dependent hazard for the SFBR's largest cities of San Francisco, Oakland, and San Jose. From hereon, what we refer to as "time-dependent hazard" in this study also contains a "time-independent" component because not all models considered by WGCEP (2003) are time-dependent. Also the hazard from the other SFBR faults is time-independent.

2. SEISMIC SOURCE INPUTS TO ANALYSIS

The SFBR is a seismically active region that sits astride the North America-Pacific plate boundary as manifested by the San Andreas fault system (Figure 1). A total of 15 earthquakes of **M** ≥ 6.0 have occurred in the SFBR since 1800 (Figure 2). Notable historical events include the 1838 **M** 6.8 San Francisco Peninsula, 1868 **M** 6.8 East Bay, 1906 **M** 7.9 San Francisco, and 1989 **M** 6.9 Loma Prieta earthquakes. The paleoseismic record, though admittedly incomplete, indicates at least 50 moderate to large earthquakes on the major faults in the past several thousand years (D.P. Schwartz, USGS, written communication, 2008). The rate of seismicity in the SFBR was higher prior to the 1906 earthquake for at least 70 years than in the century following the earthquake. The current thinking is that the 1906 earthquake relieved much of the regional stress accumulation leaving the SFBR in its "stress shadow" (WGCEP, 2003). This stress shadow is a significant factor in estimating the future occurrence of large earthquakes and the associated hazard.

Seismic source characterization is concerned with three fundamental elements: (1) the identification, location, and geometry of significant sources of earthquakes; (2) the maximum size of the earthquakes associated with these sources; and (3) the rate at which they occur. In this study, the dates of past earthquakes on specific faults are required in addition to the frequency of occurrence. The source parameters for the significant faults in the SFBR (Figure 1) are characterized for input into the PSHA. Areal source zones using the historical seismicity record are used in the PSHA to account for the hazard from background earthquakes.

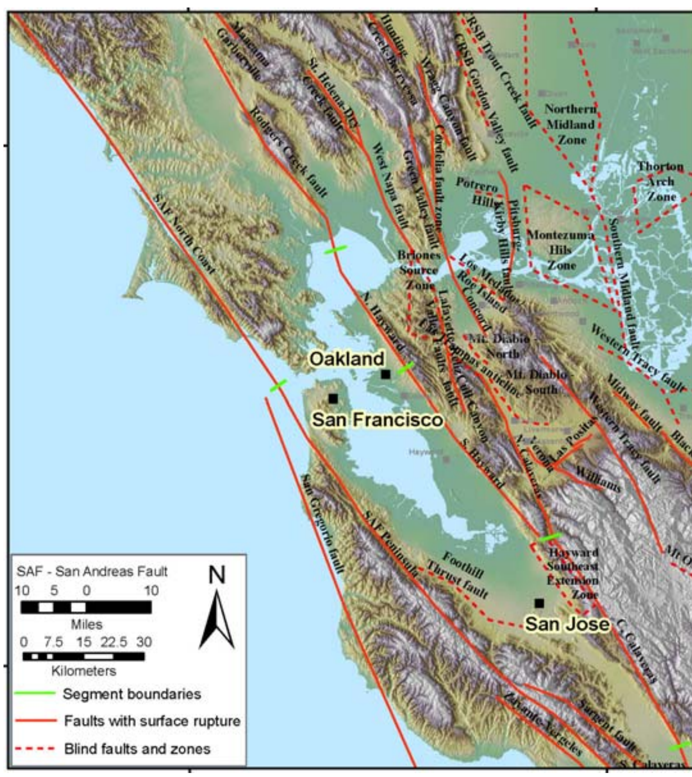

Figure 1. Active Faults in the San Francisco Bay Region

The fundamental seismic source characterization in this study came from studies performed by the USGS Working Group on Northern California Earthquake Potential (WGNCEP, 1996), the WGCEP (2003), and the California Geological Survey's seismic source model used in the USGS National Hazard Maps (Cao et al., 2003). This characterization was updated and revised based on recent research (Wong et al., 2008). Uncertainties in the seismic source parameters were incorporated into the PSHA using logic trees.

WGCEP (2003) describes and summarizes the current understanding of the major SFBR faults. In their analyses to estimate earthquake probabilities along the major faults, the WGCEP (2003) used models that are time-dependent, i.e., they account for the size and time of the last earthquake. The time-dependent earthquake probability models were used directly with computer codes obtained from the USGS to obtain rates of characteristic events for the seven major SFBR faults considered by WGCEP (2003): San Andreas, Hayward/Rodgers Creek, Calaveras, Concord/Green Valley, San Gregorio, Greenville, and Mt. Diablo (Table 1). All other faults considered in the PSHA were modeled with a Poisson model due to the lack of data to characterize time dependence. The seismic source parameters of these faults are described in Wong et al. (2008).

The WGCEP (2003) model consists of numerous rupture sources (i.e., a single fault segment or combination of two or more adjacent segments that produce an earthquake) (Table 1). For instance, the Greenville fault source has three rupture sources, a southern segment (GS), northern segment (GN), and unsegmented (GS+GN). A rupture scenario is a combination of rupture sources that describe complete failure of the entire fault, i.e., for the Greenville fault there are three scenarios: GN and GS rupture independently, GN+GS, and a floating rupture along GN+GS (Table 1). Fault rupture models are the weighted combinations of the fault-rupture scenarios. These weights were determined considering what would be the frequency (percentage) of each rupture scenario if the entire length of the fault failed completely 100 times. These weights are adjusted slightly to account for moment balancing. The rupture scenarios and adjusted model weights provide the long-term mean rate of occurrence of each rupture source for each of the characterized faults. The WGCEP (2003) approach described above differs from the logic tree characterization used in typical time-independent hazard analyses. Rupture scenarios in the WGCEP (2003) model are treated as an aleatory variable. The members of WGCEP (2003) were asked to consider the distribution of the rupture scenarios for each fault. Logic trees characterize rupture scenarios as epistemic uncertainty, with each rupture scenario given a weight representing an estimate of how likely it is the actual rupture scenario.

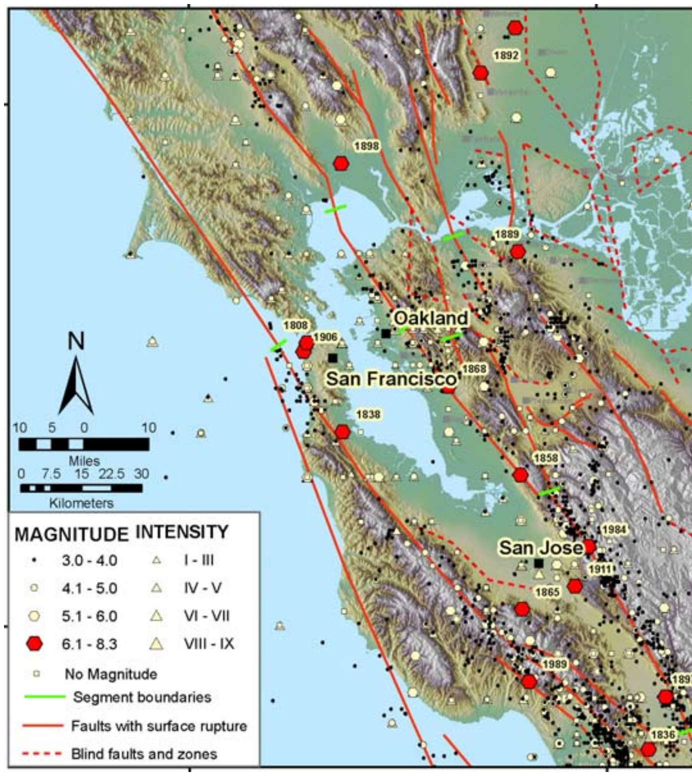

Figure 2. Historical Seismicity (1800 to 2008) in the San Francisco Bay Region

In calculating earthquake probabilities in the SFBR, WGCEP (2003) recognized two important aspects that affect earthquake occurrence: the earthquake cycle, which centers on the strain accumulation associated with the 1906 earthquake, and fault interactions. The time-dependent hazard is calculated using the range of earthquake probability models that were considered by WGCEP (2003). They considered five probability models that account for various degrees of physics, date of last rupture, recent seismicity rates, and slip in the 1906 earthquake: Poisson, Empirical, Brownian Passage Time (BPT), BPT-step, and Time-Predictable (TP) (Table 2). The Empirical model is a variation of the Poisson model. It incorporates time dependence by modulating the average rates of rupture sources with the current rate of seismicity (WGCEP, 2003). Because the SFBR is emerging out of the 1906 stress shadow, the current seismicity rate is lower than the long-term average. The BPT time-dependent model specifies the failure condition of a fault or fault segment by a state variable that rises from a ground state to failure state during the earthquake cycle (WGCEP, 2003). A variation of the BPT model is the BPT-step that allows steps in the state variable calculated with elastic interaction models. The well-established TP model, which is only

Table 1. SFBR Fault Time-Dependent Seismic Source Parameters in 2005

Fault	**Segments**	**Rupture Length (km)**	**Preferred Magnitude (M)**	**Mean Characteristic Event Rate**
San Andreas	Santa Cruz Mountains (SAS)	62	7.03	1.79×10^{-3}
	Peninsula (SAP)	85	7.15	5.60×10^{-3}
	North Coast (SAN)	191	7.45	9.31×10^{-4}
	Offshore (SAO)	135	7.29	8.87×10^{-4}
	SAS + SAP	147	7.42	3.22×10^{-3}
	SAN + SAO	326	7.70	2.95×10^{-3}
	SAS + SAP + SAN	338	7.76	8.98×10^{-3}
	SAP + SAN + SAO	411	7.82	2.82×10^{-4}
	SAS + SAP + SAN + SAO	473	7.90	4.25×10^{-3}
	Floating Earthquake	N/A	6.90	6.49×10^{-3}
Hayward – Rodgers Creek	Southern Hayward (HS)	53	6.67	1.08×10^{-2}
	Northern Hayward (HN)	35	6.49	1.46×10^{-2}
	HS + HN	88	6.90	8.65×10^{-3}
	Rodgers Creek (RC)	63	6.98	1.44×10^{-2}
	HN + RC	98	7.11	2.34×10^{-3}
	HS + HN + RC	151	7.26	1.11×10^{-3}
	Floating Earthquake	N/A	6.90	4.80×10^{-4}
Calaveras	Southern Calaveras (CS)	19	5.79	3.77×10^{-2}
	Central Calaveras (CC)	59	6.23	1.80×10^{-2}
	Northern Calaveras (CN)	45	6.78	1.45×10^{-2}
	CS + CC	78	6.36	7.92×10^{-3}
	CC + CN	104	6.91	1.00×10^{-3}
	CS + CC + CN	123	6.94	2.81×10^{-3}
	Floating Earthquake	N/A	6.20	6.66×10^{-3}
San Gregorio	Southern San Gregorio (SGS)	66	6.96	3.09×10^{-3}
	Northern San Gregorio (SGN)	110	7.23	5.03×10^{-3}
	SGS + SGN	176	7.44	2.93×10^{-3}
	Floating Earthquake	N/A	6.90	1.23×10^{-3}
Greenville	Southern Greenville (GS)	24	6.60	2.80×10^{-3}
	Northern Greenville (GN)	27	6.66	2.82×10^{-3}
	GS + GN	51	6.94	1.29×10^{-3}
	Floating Earthquake	N/A	6.20	2.73×10^{-4}
Concord – Green Valley	Concord (CON)	20	6.25	5.70×10^{-3}
	Southern Green Valley (GVS)	22	6.24	2.85×10^{-3}
	CON + GVS	42	6.58	2.00×10^{-3}
	Northern Green Valley (GVN)	14	6.02	7.05×10^{-3}
	GVS + GVN	36	6.48	3.78×10^{-3}
	CON + GVS + GVN	56	6.71	7.37×10^{-3}
	Floating Earthquake	N/A	6.20	1.07×10^{-2}
Mt. Diablo	Mt. Diablo	31	6.65	6.72×10^{-3}

applied to the San Andreas fault (Table 2), models the expected time of the next "characteristic" earthquake based upon the amount of slip and date of the most recent event. Detailed slip data for the other major faults are lacking to apply the TP model.

WGCEP (2003) applied weights to these five models for each of the seven major faults it considered (Table 2). The five probability models and their weights were used to compute the rates of characteristic events on each rupture source (Table 1), which were then used in the PSHA. For this study, rupture probabilities were calculated for 1-year exposure windows for the year 2005.

Table 2. Mean Expert Weights for Probability Models Applied to the Major SFBR Faults (Table 5.5, WGCEP, 2003)

Fault System	Poisson	Empirical	BPT	BPT-Step	Time-Predictable
San Andreas	0.100	0.181	0.154	0.231	0.335
Hayward/Rodger’s Creek	0.123	0.285	0.131	0.462	—
Calaveras	0.227	0.315	0.142	0.315	—
Concord/Green Valley	0.246	0.277	0.123	0.354	—
San Gregorio	0.196	0.292	0.115	0.396	—
Greenville	0.231	0.288	0.131	0.350	—
Mt. Diablo Thrust	0.308	0.396	0.092	0.204	—

Modifications to the WGCEP (2003) inputs were made to accommodate their use in PSHA. The program for computing the time-predictable probabilities for the San Andreas rupture scenarios was obtained from Dr. William Ellsworth, USGS. The Empirical model of Reasenberg et al. (2003) was used to obtain the scale factors to modify the long-term rate. WGCEP (2003) used Reasenberg et al. (2003) models A through F and assigned weights of 0.1, 0.5, and 0.4 to the minimum, average, and maximum scale factor, respectively. The only modifications made for the Poisson, BPT and BPT-step model inputs were to change the exposure time to 1 year and to compute results for 2005.

The hazard code requires the activity rate of all events above the minimum magnitude and the rate of characteristic events (Table 1). This activity rate is used along with the normalized magnitude probability density function (pdf) to describe the rate of all magnitudes of events on the rupture source. The activity rates were calculated by scaling up the normalized magnitude pdf such that the rate of characteristic events matched the rate provided by the WGCEP (2003) model. The mean, 5th, and 95th percentile rates of characteristic events for each rupture source provided by the WGCEP (2003) model were input into the hazard code, along with the source geometries, characteristic magnitudes, and shape of the magnitude distributions. The characteristic event is defined by a normal distribution truncated at the upper and lower ends at 2*sigma, where sigma is 0.12 magnitude units. A portion of the moment rate of the fault is accounted for with an exponential tail of smaller events, defined by a *b*-value. WGCEP (2003) used a mean value of 6% of moment rate in the exponential tail, along with branches that used 4% and 8% with lower weights. For simplicity, a single value of 6% of the moment rate was applied to the exponential tail in the PSHA.

3. GROUND MOTION ATTENUATION RELATIONS

The new attenuation relationships for tectonically-active regions developed as part of the Next Generation of Attenuation (NGA) Project sponsored by the Pacific Earthquake Engineering Research (PEER) Center were used in the PSHA. The relationships by Chiou and Youngs (2008), Campbell and Bozorgnia (2008), Boore and Atkinson (2008), and Abrahamson and Silva (2008) have a substantially better scientific basis than previous models. These relationships were derived from a significantly expanded strong motion database that includes records from the 1999 **M** 7.5 Kocaeli and **M** 7.1 Duzce, Turkey, and 2001 **M** 7.6 Chi Chi, Taiwan earthquakes. The relationships were weighted equally in the PSHA. An average shear-wave velocity in the top 30 m (V_S30) of 270 m/sec for a firm soil condition was used in the NGA models. Forward rupture directivity was also incorporated into the PSHA using the models of Somerville et al. (1997) and Abrahamson (2000).

4. TIME-DEPENDENT PSHA RESULTS

The results of the time-dependent PSHA of San Francisco, Oakland, and San Jose are presented in terms of ground motion as a function of annual exceedance probability or average return period. Figures 3 to 5 show the mean hazard curves for peak horizontal acceleration (PGA) for the three cities. The probabilistic PGA and 1.0 sec horizontal spectral accelerations (SA) are listed in Table 3 for the typical building code return periods of 475 and 2,475 years for the year 2005 (10% and 2% exceedance probabilities in 50 years, respectively). Figures 3 to 5 also show the time-independent hazard for PGA.

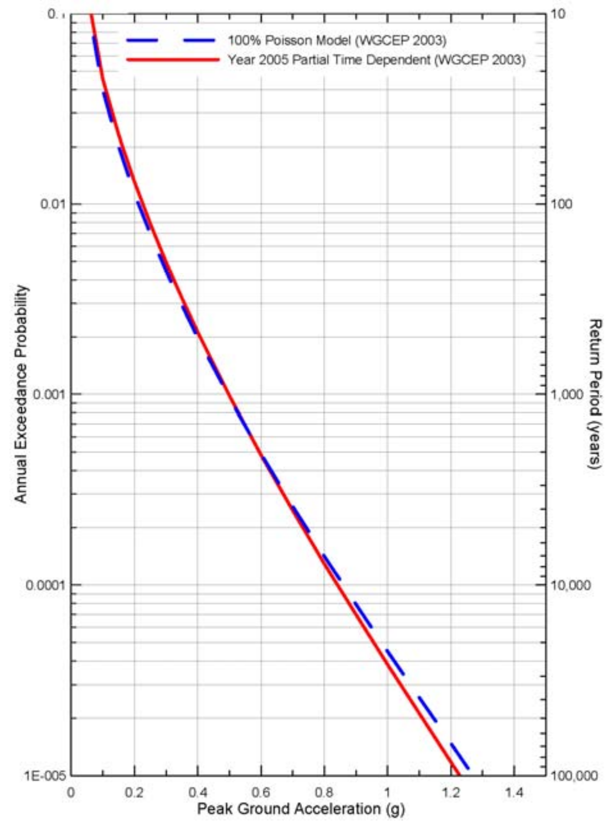

Figure 3. Time-Independent and Time-Dependent Mean Hazard Curves for San Francisco

The hazard in San Francisco is controlled by the San Andreas fault because of its proximity to the fault (Figure 1). Oakland in contrast is traversed by the Hayward fault and so the hazard is controlled by that fault (Figure 1). San Jose is located between the San Andreas fault and the Hayward-Calaveras fault junction. The time-dependent PGA hazard is very similar to the time-independent hazard in downtown San Francisco because in part the elapsed time since the 1906 earthquake has only been about 100 years, much shorter than the average recurrence interval of 180 to 370 years for 1906-type events (WGCEP, 2003). At return periods longer than 2,500 years, the time-independent PGA hazard in 2005 actually exceeds the time-dependent hazard as the San Andreas fault contribution to the hazard becomes more dominant (Figure 3). In contrast, in Oakland the time-dependent hazard is higher by about 5 to 10% than the time-independent PGA hazard because the elapsed time since the most recent earthquake in 1868 is nearly the same as the average recurrence interval of 140 years (Figure 4). The small increase in hazard going from the time-independent to time-dependent hazard seems small to almost negligible (Table 3), but note there is about 10 to 30% Poissonian component to the time-dependent hazard calculations (Table 2). Finally, the time-dependent PGA hazard in San Jose is nearly identical to the time-independent hazard (Figure 5). There are several nearby faults including the thrust faults at the southern end of the Hayward fault, the Hayward fault itself, and the Calaveras and San Andreas faults that are contributing to the hazard in San Jose and so differences between the time-independent and time-dependent are not expected.

Table 3. Summary of Time-Dependent and Time-Independent Hazard

Return Period	**PGA (g's)**				**1.0 Sec SA (g's)**			
	475 years		**2,475 years**		**475 years**		**2,475 years**	
City	**TD**	**TI**	**TD**	**TI**	**TD**	**TI**	**TD**	**TI**
San Francisco	0.40	0.39	0.63	0.63	0.53	0.53	0.95	0.97
Oakland	0.49	0.45	0.77	0.72	0.64	0.59	1.12	1.04
San Jose	0.47	0.46	0.72	0.71	0.60	0.58	1.01	0.99

TD = Time-dependent, TI = Time-independent

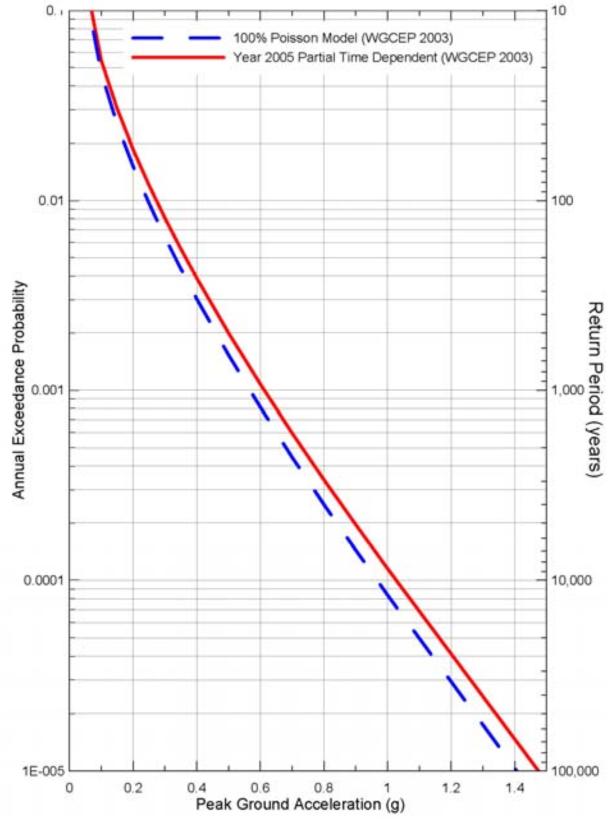

Figure 4. Time-Independent and Time-Dependent Mean Hazard Curves for Oakland

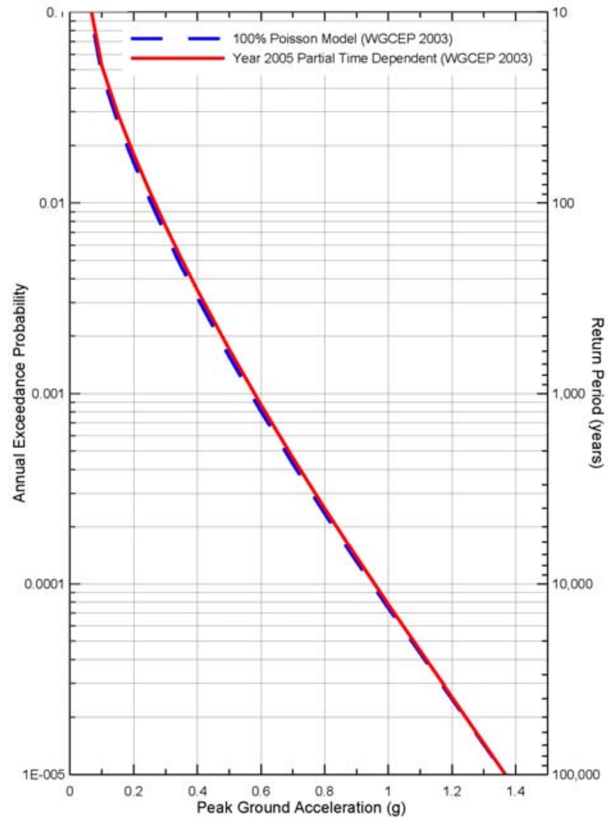

Figure 5. Time-Independent and Time-Dependent Mean Hazard Curves for San Jose

5. SUMMARY

The small differences observed between the time-dependent and time-independent hazard in the SFBR based on the results of WGCEP (2003) reflects, to a large extent, the probability models used in their analyses and the inclusion of a significant Poisson component. Despite a century of research, there remain considerable uncertainties in the characterization of the major faults in the SFBR and this is reflected in the WGCEP (2003) assessments. In particular, there was no consensus within WGCEP (2003) on whether the SFBR remains within the 1906 stress shadow, is now emerging out of it, or is already out of the shadow. This is a significant uncertainty that is reflected in the probability model selection and their weights. Although in aggregate, the probability of a large earthquake in the SFBR is relatively high at 62%, the time-dependent hazard is really no different than the time-independent hazard on a site-specific basis. This is because in general, large parts of the region are governed by a single controlling fault and the probability of a large earthquake on any individual fault from 2002 to 2031 does not exceed 30%.

6. ACKNOWLEDGMENTS

This study was partially supported by the California Department of Water Resources as part of the Delta Risk Management Strategy Project. Our thanks to Melinda Lee, Deb Fournier, and Fabia Terra for their assistance in the preparation of this paper, and to Keith Knudsen for his review.

7. REFERENCES

Abrahamson, N. (2000). Effects of rupture directivity on probabilistic seismic hazard analysis. Sixth International Conference on Seismic Zonation **I**, 151-156.

Abrahamson, N.A. and Silva, W.J. (2008). Summary of the Abrahamson and Silva NGA ground motion relations. *Earthquake Spectra* **24**, 67-97.

Boore, D.M. and Atkinson, G.M. (2008). Ground motion predictive equations for the average horizontal component of PGA, PGV, and 5% damped PSA at spectral periods between 0.01s to 10.0s. *Earthquake Spectra* **24**, 99-138.

Cao, T., Bryant, W.A, Rowshandel, B., Branum, D., Wills. C.J. (2003). The revised 2002 California probabilistic seismic hazard maps, June 2003. California Geological Survey, http://www.consrv.ca.gov/CGS/rghm/psha/fault_parameters/ pdf/2002_CA_Hazard_Maps.pdf.

Campbell, K.W. and Bozorgnia, Y. (2008). NGA ground motion model for the geometric mean horizontal component of PGA, PGV, PGD, and 5% damped linear elastic response spectra for periods ranging from 0.01 to 10 s. *Earthquake Spectra* **24**, 139-171.

Chiou, B.S.J. and Youngs, R.R. (2008). An NGA model for the average horizontal component of peak ground motion and response spectra. *Earthquake Spectra* **24**, 173-215.

Reasenberg, P.A., Hanks, T.C., and Bakun, W.H. (2003). An empirical model for earthquake probabilities in the San Francisco Bay region, California, 2002-3031. *Bulletin of the Seismological Society of America* **93**, 1-13.

Somerville, P.G., Smith, N.F., Graves, R.W., and Abrahamson, N.A. (1997). Modification of empirical strong ground motion attenuation relations to include the amplitude and duration effects of rupture directivity. *Seismological Research Letters* **68**, 199-222.

Wong, I., Thomas, P., Unruh, J., Hanson, K., and Youngs, R. (2008). Characterizing the earthquake ground shaking hazard in the Sacramento-San Joaquin Delta, California. Fourth Decennial Geotechnical Earthquake Engineering and Soil Dynamics Conference.

Working Group for California Earthquake Probabilities (WGCEP) (2003). Earthquake probabilities in the San Francisco Bay area: 2002-2031. U.S. Geological Survey Open-File Report 03-214.

Working Group on Northern California Earthquake Potential (WGNCEP) (1996). Database of potential sources for earthquakes larger than magnitude 6 in northern California. U.S. Geological Survey Open-File Report 96-705, 53 p.